PAN POLSKA AKADEMIA NAUK

METROLOGY AND MEASUREMENT SYSTEMS

Index 330930, ISSN 0860-8229

www.metrology.pg.gda.pl

M&MS

MACHINE LEARNING SYSTEM FOR AUTOMATED BLOOD SMEAR ANALYSIS

Michał Grochowski[1)], Michał Wąsowicz[2)], Agnieszka Mikołajczyk[1)], Mateusz Ficek[3)], Marek Kulka[2)], Maciej S. Wróbel[3)], Małgorzata Jędrzejewska-Szczerska[3)]

1) *Gdańsk University of Technology, Faculty of Electrical and Control Engineering, G. Narutowicza 11/12, 80-233 Gdańsk, Poland* (✉ *michal.grochowski@pg.edu.pl*, +48 58 347 2904, *agnieszka.mikolajczyk@pg.edu.pl*)
2) *Warsaw University of Life Sciences, Faculty of Veterinary Medicine, Nowoursynowska 159, 02-776 Warsaw, Poland* (*michal_wasowicz@sggw.pl*, *marek_kulka@sggw.pl*)
3) *Gdańsk University of Technology, Faculty of Electronics, Telecommunications and Informatics, G. Narutowicza 11/12, 80-233 Gdańsk, Poland* (*matficek@pg.edu.pl*, *maciej.wrobel@pg.edu.pl*, *malszcze@pg.edu.pl*)

Abstract

In this paper the authors propose a decision support system for automatic blood smear analysis based on microscopic images. The images are pre-processed in order to remove irrelevant elements and to enhance the most important ones – the healthy blood cells (erythrocytes) and the pathologic ones (echinocytes). The separated blood cells are analysed in terms of their most important features by the eigenfaces method. The features are the basis for designing the neural network classifier, learned to distinguish between erythrocytes and echinocytes. As the result, the proposed system is able to analyse the smear blood images in a fully automatic way and to deliver information on the number and statistics of the red blood cells, both healthy and pathologic. The system was examined in two case studies, involving the canine and human blood, and then consulted with the experienced medicine specialists. The accuracy of classification of red blood cells into erythrocytes and echinocytes reaches 96%.

Keywords: optical microscopy, blood cells, biophotonics, image analysis, classification, eigenfaces, neural networks, decision support, nanodiamonds, bioimaging.

1. Introduction

Blood testing is one of the most common diagnostic tools used in monitoring human and animal health and in diagnosing diseases. It depends on the qualitative and quantitative assessment of blood morphological elements. It is always analysed based on commonly accepted standards depending on age and sex, supplemented by well-collected interviews and medical examinations [1, 2]. Currently, research is underway to develop an alternative method of analysing saliva or hair. These methods of examination will not, however, replace the morphological evaluation of blood due to lower accuracy. Still, examination of blood is an important part of prophylaxis and thus enables rapid detection of possible abnormalities in the body. One of the most commonly used methods of blood examination is to analysing its smear image [3]. With the smear image analysis, it is possible to evaluate morphological features of blood cells such as: colour, shape, size *etc*. One can observe normal and pathologic erythrocytes in the blood smears where red blood

Article history: received on May 07, 2018; accepted on Oct. 10, 2018; available online on Mar. 29, 2019, DOI: 10.24425/mms.2019.126323.

cells have an oval shape of similar diameter. The detection of abnormal conditions is related to changes in the colour, shape and size of red blood cells [1–3].

The use of optical methods for blood testing, based on processing microscopic images, is still an object of interest to researchers, primarily due to the continuing lack of simple and inexpensive blood testing devices. The previous studies have suggested a variety of methods for blood cells' segmentation, counting and classification, but the majority of papers are focused only on segmentation and counting. The authors of [4–11] proposed a method of detecting and counting *red blood cells* (RBC) as well as *white blood cells* (WBC). They reached respectively: accuracy of 95.3% for RBC count and 98.4% for WBC count by using an iterative-structured circle-detection algorithm; 95.5% of overall accuracy by using a merged method of k-means clustering, Sobel edge detection and watershed transform; high accuracy by using a distance-transformed watershed. The authors of [8] reported 95.9% accuracy and 97.99% sensitivity obtained with the use of a line operator and a watershed algorithm, respectively. Another type of approach to automation of blood smear analysis was differentiating of all lymphocytes using grey-level co–occurrence matrices and shape-based features, which reached accuracy of 89.8% [9]. In [10] the authors have focused on WBCs' segmentation by colour-space-based k-means clustering and reached 95.7% and 91.3% overall accuracy for nucleus segmentation and cytoplasm segmentation, respectively. Another interesting paper [11] presents an image processing and analysis methodology using supervised classification to assess the presence of malaria parasites and to determine the species and life-cycle stage in Giemsa-stained thin blood smears. Eight different species-stage combinations were considered, with sensitivity from 73.9% to 96.2% and specificity from 92.6% to 99.3%. Nowadays, technical solutions such as biomedical imaging [5–14] and optoelectronic sensors [15–17] have become powerful tools for diagnostics of human and animal health condition.

In this paper the authors propose a computer-aided decision-support system for RBC counting, but – in contrary to other papers – also for classification of RBCs into the normal and pathologic ones. In the pre-processing stage, a number of morphological and arithmetical operations are executed over the images, the main obstacles are erased from the images and the RBCs are separated. In order to detect and count the pathologic erythrocytes, the most important features of the blood cells are extracted by the eigenfaces algorithm, a common computer-vision algorithm originally developed for the purpose of facial recognition [18]. This method also significantly reduces the numerical representation of RBCs, enabling effective and efficient application of a neural network as the classifier. Finally, the classification process is carried out by skilfully trained neural networks that are well suited for such kind of problems [19–22], also in other applications.

The system capability to support the classification of blood cells was examined on a group of blood cells incubated with nanodiamonds. The incubation of blood cells with nanoparticles introduces some changes in their morphology which gives us the opportunity to differentiate the normal and abnormal cells.

Our previous study [23] focused on assessment of the haemo-compatibility of nanodiamonds in respect of red blood cells, and was performed on several types of nanodiamonds. The assessment was carried out by trained physicians analysing peripheral blood smears. Therefore, this paper uses the data from our previous study on the human blood, with addition of new data, obtained following the identical protocol, but for the canine blood. This is a step towards development of novel medical tools, also in veterinary medicine. Specific medical goals to be achieved with the utilization of nanodiamonds include drug delivery through blood-brain barrier, bio-imaging and bio-sensing. This is further discussed in our previous paper [23]. Specific modifications of nanodiamonds, mostly their surface chemistry, may be the crucial factors which decide whether such nanoparticles can be, in future, applied in vivo. Therefore, any modifications require haemo-compatibility testing, for which purpose this automated blood smear analysis system is developed.

2. Materials and methods

2.1. Data acquisition of healthy and nanodiamond-affected red blood cells

This study uses two sets of microscopic images of erythrocytes from blood smears of both human (from [23]) and canine species. One group consists of normal discoid red blood cells (human N_{Hh} = 5893; canine N_{Ch} = 1350) and the other – abnormal cells (human N_{Hp} = 147; canine N_{Cp} = 18), both affected by addition of nanodiamonds. The authors have followed the exact procedures in the same way as in the previous research on nanodiamonds' haemo-compatibility [23], where the procedures are described in full detail. Briefly, the human and canine venous blood samples were collected from healthy individuals into tubes with EDTA. Some blood samples were incubated with *nanodiamond solutions* (NDs). A *complete blood count* (CBC) test and a stained blood smear analysis were performed and the results were compared with those obtained for the blood samples without NDs (controls). The suspended nanodiamonds (1000 ng/μL) were introduced into 500 μL aliquots of the blood samples in two concentrations, resulting in concentrations of about 38 ng/μL and 167 ng/μL of NDs in the blood samples. The samples were incubated up to specified time points, and the blood stains were performed after each time point. At least 10 blood stains were always performed for each sample from at least 10 volunteers. The blood smears were stained according to the *May-Grünwald and Giemsa* (MGG) staining procedure [24, 25]. The classification of cells was concluded as previously, by a trained physician after examination of the peripheral blood slides. In the following studies, the presence of individual cells differing in the cell membrane shape has been detected. Cells with regularly spaced blunt or pointed projections of the same size were classified as echinocytes. These cells are present in dehydrated individuals and patients with renal failure, diabetes mellitus and lymphoma. Echinocytes could be also an artefact in vitro due to either a prolonged blood storage or as a result of excess EDTA to the collected blood volume.

2.2. Decision support system – idea

The blood smear evaluation is an important method used in the diagnostic process, however it is time-consuming and in some cases affected by a human error. The main problems of automated evaluation in a correct analysis of red blood cells are overlapping platelets and sometimes white blood cells. Examples of human and canine blood microscopic smear images are shown in Fig. 1.

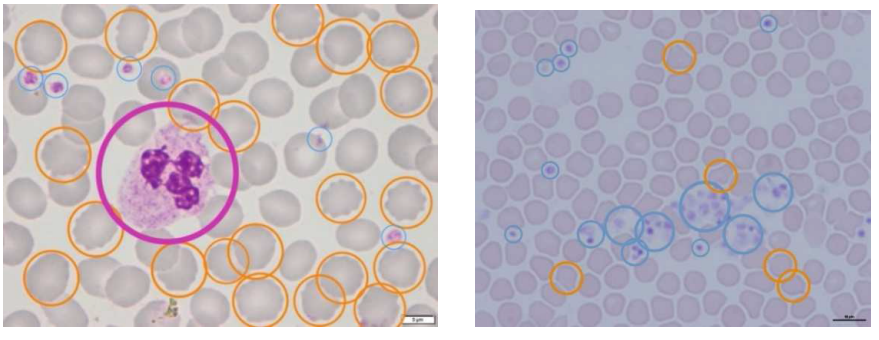

Fig. 1. Examples of human (left) and canine (right) microscopic stained blood.
Orange circles indicate pathologic erythrocytes, blue – platelets and pink – white blood cells.

The problem of computer-aided automatic counting of red blood cells has been approached several times. In this paper the authors propose a computer-aided system for counting the red blood cells as well as their classification into groups of normal and pathological ones. The described system pre-processes the images in order to separate the blood cells, assess cell counts and afterwards classify the RBCs as normal (erythrocytes) or pathologic (echinocytes) ones. Finally, the results of counting and classification are obtained (accuracy, sensitivity, specificity). A flowchart explaining the main steps carried out by the system is shown in Fig. 2.

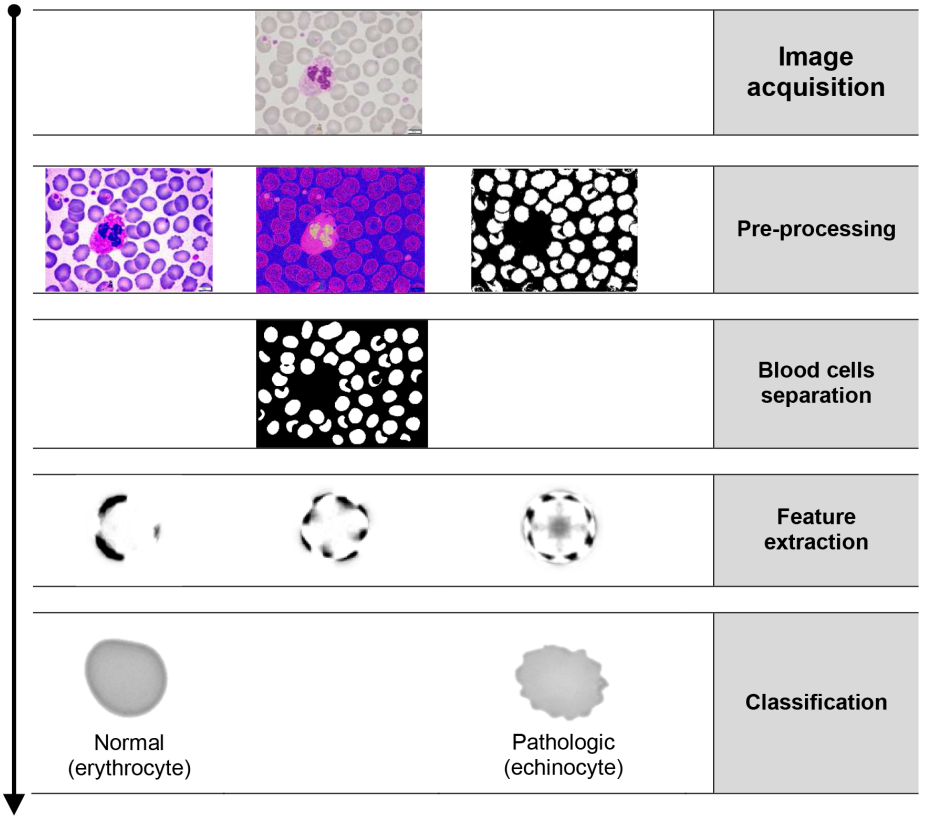

Fig. 2. A flowchart of the classification process.

2.3. Separation of cells

The microscopic images of a blood smear are loaded by the image processing system in the RGB format (Red, Green, Blue channels). In order to separate the red blood cells, a number of operations on an image are carried out. Firstly, saturation of the image, as well as contrast in G channel are increased by equalization of the histogram. Then, in R channel, brightness is reduced and contrast is enhanced. In order to remove the background noise and to highlight the centres of erythrocytes, the morphological operations like dilatation and erosion are applied. They enable the visual separation of the overlapping cells. To isolate the white blood cells from the platelets, the image is converted into HSV colour space, then blurred, and its contrast is increased. By subtracting the V image layer from the S layer in the HSV colour space, the grey-

scale image is obtained in which contours of platelets, white blood cells and erythrocytes are clearly visible. Then, the morphological closing is carried out in order to fill up holes in the image, and the morphological opening – to erase too small objects. Finally, the algorithm determines the coordinates of centroids and the radii of objects and counts them, afterwards. The algorithm steps and the final result are presented in Fig. 3.

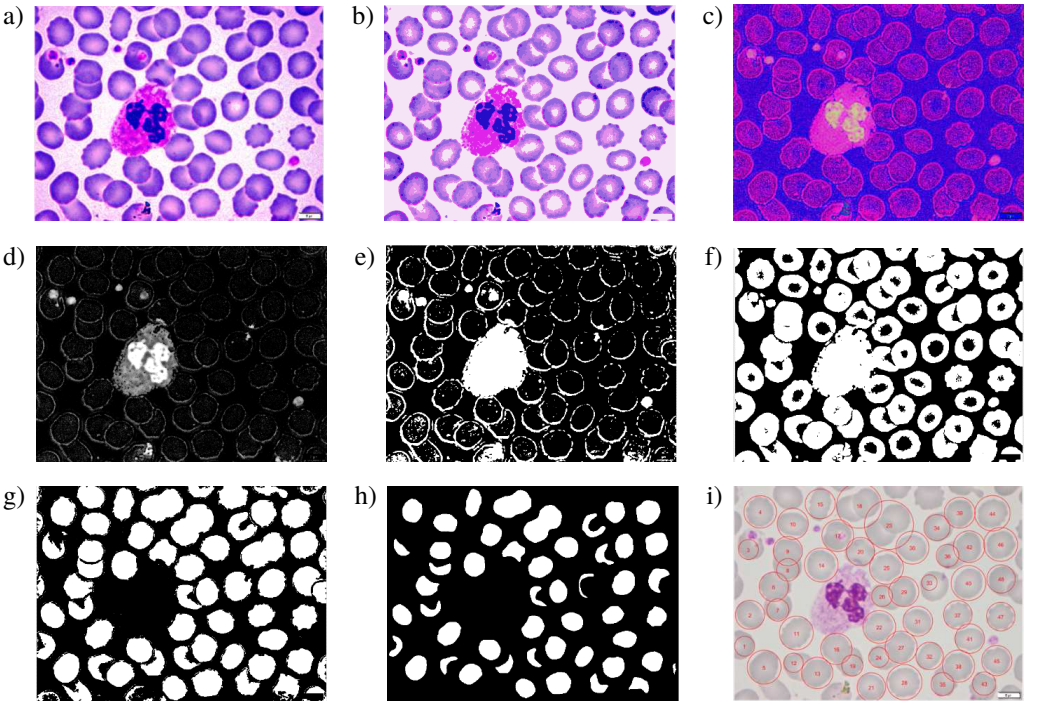

Fig. 3. Successive steps of the RBC counting algorithm: a) Step 1; b) Step 2; c) Step 3; d) Step 4; e) Step 5; f) Step 6; g) Step 7; h) Step 8; i) Step 10.

The algorithm of RBC separation and counting:

- **Step 1:** Reading the image in RGB format (Fig. 1); increasing saturation of the image; increasing contrast in G channel by equalization of the histogram; reducing brightness and increasing contrast in R channel (see Fig. 3a).
- **Step 2:** Applying the morphological operations: dilatation and erosion (Fig. 3b).
- **Step 3:** Conversion of the image to the HSV colour space; image blurred; increasing contrast (Fig. 3c).
- **Step 4:** Subtracting V layer from S layer of the image in the HSV colour space (Fig. 3d).
- **Step 5:** Thresholding the image from Step 4 (Fig. 3e).
- **Step 6:** Thresholding the image from Step 2 (Fig. 3f).
- **Step 7:** Subtracting the image from Step 6, from the image from Step 5 (Fig. 3g).
- **Step 8:** Filling holes (morphological closing) in the image and deleting small objects (Fig. 3h).
- **Step 9:** Determining the coordinates of centroids and the radii of objects in the image from Step 8.
- **Step 10:** Applying the circles determined in Step 9 to the original image and counting (Fig. 3i).

The described above steps enable automatic separation of the erythrocytes, which are analysed afterwards for the presence of pathologic blood cells (echinocytes). Examples of erythrocytes extracted from the image are shown in Fig. 4. It should be noticed that the erythrocytes and echinocytes differ only in the edge shapes of the cells.

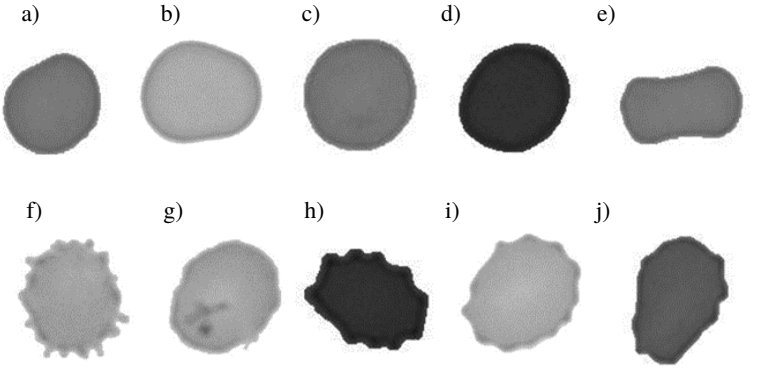

Fig. 4. Examples of red blood cells extracted from the image: a)–e)erythrocytes, f)–j) echinocytes.

2.4. Detection of pathologic erythrocytes in blood smear

RBCs extracted from the blood smear images are the base for training the classifier, in this case a neural network. However, the extracted blood cells have a 100×100 size, what results in a vector for classification of a 10 000 size for each cell, making the training process inefficient or just impossible. In order to significantly decrease the image size to make the classification much easier and to extract the most characteristic features of the blood cells at the same time, the Eigenfaces [18] method was applied. This method is very popular in computer vision for the purpose of facial recognition but it has features that are very beneficial in this case.

2.4.1. Eigenfaces method

The Eigenfaces method enables to describe an original image by a much smaller set of representative images called eigenfaces. The algorithm is based on *Principal Component Analysis* (PCA) [27, 28] and the mentioned eigenfaces are the two-dimensional equivalents of the eigenvectors in PCA, hence are easily applicable to the image processing. The eigenfaces, originally developed for facial recognition, can be considered as a set of standardized elements of a face, obtained from the statistical analysis of many faces. Then, any single face can be reconstructed as a linear combination of these eigenfaces plus the average image of face. The number of eigenfaces used in order to approximate the original image is the main parameter to be found.

In the problem considered in this paper, it is the red blood cells (normal and pathologic) that are to be analysed by the algorithm instead of the human faces. The goal is to extract the most important features distinguishing the normal red blood cells (erythrocytes) from the pathologic ones (echinocytes) and to reduce the size of vectors describing the cells at the same time. As a result, the grey-scale blood cell images of a 100×100 size are transformed into eigenvectors $u_1 - u_k$ representing the most important cell features, of $k = 30$ size, in this case. These vectors are presented in Fig. 5. Next, by a number of linear transformations [18, 27, 28] a weight ω_k of the k-th eigenface needs to be found. Hence, each of the images is represented by weight

vectors $\Omega = [\omega_1, \omega_2, \ldots, \omega_k]$. The reconstructed image is a linear combination of the eigenfaces (eigenbloodcells) u_1–u_k and the weight vector Ω, plus the average image. The reconstruction process of the original images with the eigenfaces method is illustrated in Fig. 5 while the algorithm itself is presented in Subsection 2.4.2.

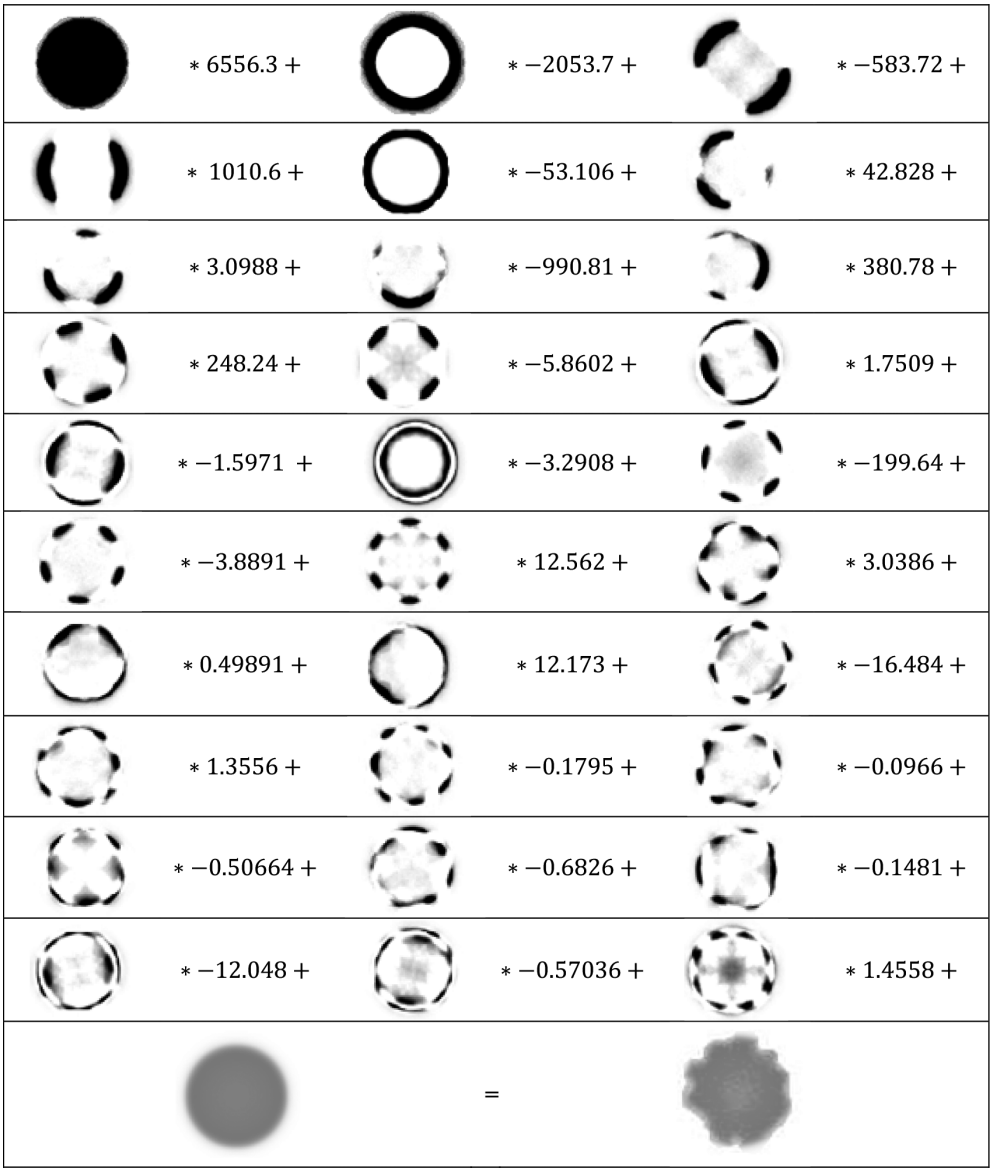

Fig. 5. An example of reconstruction of a red blood cell by using the eigenfaces method. The top left eigenface (eigenbloodcell) is the most while the bottom right is the least important one. The reconstructed blood cell (bottom right) is a linear combination of eigenfaces (eigenbloodcells) and the corresponding weight vector $\acute{\Omega}$ plus an average image (bottom left). $\acute{\Omega}$ = [6556.3, −2053.7, −583.72, 1010.6, −53.106, 42.828, 3.0988, −990.81, 380.78, 248.24, 5.8602, 1.7509, −1.5971, −3.2908, −199.64, −3.8891, 12.562, 3.0386, 0.49891, 12.173, −16.484, 1.3556, −0.1795, −0.0966, −0.50664, −0.6826, −0.1481, −12.048, −0.57036, 1.4558].

2.4.2. Neural networks

The goal of the algorithm is to decide whether the analysed erythrocytes have a normal or pathologic structure (see Fig. 1 and Fig. 4). A cell deformation may be caused by either a patient's disease or by interaction with the nanodiamonds. Due to its capability of learning from the data and generalizing the knowledge onto similar cases, a *neural network* (NN) was chosen as the classifier. The images of the separated erythrocytes pre-processed by the eigenfaces method are used to train the neural network. The successive steps of the algorithm of the decision-support system are presented below.

- **Step 1:** Read the extracted RBCs (see Fig. 1).
- **Step 2:** Apply the eigenfaces method:
- **Step 2.1:** Convert the images into the grey-scale space.
- **Step 2.2:** Subtract the mean. The average image has to be calculated and then subtracted from each original image.
- **Step 2.3:** Convert the images into vectors and form the covariance matrix.
- **Step 2.4:** Calculate eigenvectors (eigenfaces) and eigenvalues of the covariance matrix.
- **Step 2.5:** Sort the eigenvalues in the descending order and arrange the eigenvectors accordingly.
- **Step 2.6:** Select the most important (top) eigenvectors (eigenfaces).
- **Step 2.7:** Represent each image in the form of vector, as a linear combination of top. eigenvectors (eigenfaces) and the mean image in the feature space.
- **Step 3:** Design the classifier:
- **Step 3.1:** Select the structure of the neural network.
- **Step 3.2:** Train the neural networks by using the vectors representing images in the feature space.
- **Step 4:** Classify the RBCs.

An illustrative flowchart of the system is presented in Fig. 6. It should be noticed the changes in dimensions and representation of the original image during successive steps. N is the number of images of a blood smear, while M is the number of separated red blood cells (M ≫ N).

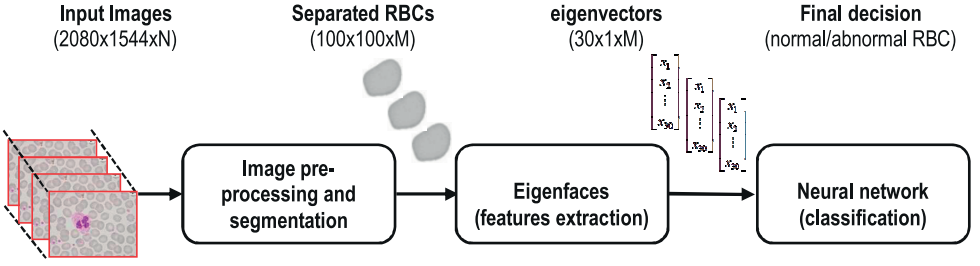

Fig. 6. A flowchart of the decision support system.

3. Results

Two case studies were considered during the research, namely analyses of the human and canine blood smears. The described computer-aided system was designed and trained to separate and then to classify the RBCs into normal and pathologic ones.

After carrying out a number of analyses and simulations, a two-layer feed-forward neural network was selected. The NN consists of 19 neurons with sigmoidal activation functions in the

hidden layer and one output neuron with a linear activation function. The network was trained to return '1' when a blood cell has a proper structure and '0' otherwise (it is pathologic) (Fig. 6).

In the case of human blood, the system was trained by using over 10000 erythrocyte images representing normal and pathologic erythrocytes. However, 6040 erythrocytes were originally taken from blood smears, while the rest were additionally created by rotation of selected original erythrocytes (up-sampling). Before the up-sampling process, all RBCs were divided into the test and training sets. Then, within each group, selected RBCs were rotated by ten degrees several times. Next, each image was copied, and each copy was flipped vertically or horizontally or both. The aim of this approach was to balance the number of normal and pathologic erythrocytes in the database, in order to increase accuracy of learning. In the up-sampling process the training set consisted of 3825 RBCs per each class, while the test set – of 1600 RBCs per class. In the case of canine blood, the problem is even greater because only about 1% of erythrocytes in the database were found to be pathologic (1350 – normal; 18 pathologic). The up-sampling process resulted in 4248 normal and 4248 pathologic red blood cells for the training set, and 1080 RBCs per class for the test set. The Levenberg-Marquardt algorithm was used as an optimizer during the neural network training.

To increase the confidence of the results, the k-fold cross-validation method was applied. The databases containing the human and canine blood cells extracted from the smear images prepared by the physicians, were randomly divided into the training and testing subsets in 5 different ways ($k = 5$).

To better evaluate the system performance, the sensitivity (TPR – *true positive rate*) and specificity (TNR – *true negative rate*) measures were calculated. The sensitivity in that case means a ratio of the properly classified echinocytes and the true number of echinocytes (1), while the specificity is a ratio of the properly classified erythrocytes and the true number of erythrocytes (2):

$$Sensitivity = \frac{TP}{P} = \frac{TP}{TP + FN}, \tag{1}$$

$$Specificity = \frac{TN}{N} = \frac{TN}{TN + FP}, \tag{2}$$

$$Accuracy = \frac{TP + TN}{P + N} = \frac{TP + TN}{TP + TN + FP + FN}, \tag{3}$$

where: P – the number of positive samples (echinocytes), N – the number of negative samples (erythrocytes), TP – True Positive: the number of echinocytes correctly identified as echinocytes; FP – False Positive: the number of erythrocytes incorrectly identified as echinocytes; TN – True Negative: the number of erythrocytes correctly identified as erythrocytes; FN – False Negative: the number of echinocytes incorrectly identified as erythrocytes.

Obviously, in medical applications, the highest sensitivity coefficient is desirable. Based on TPR and TNR measures, the ROC (*Receiver operating characteristic*) curves of classification process are drawn in Fig. 7. The *area under the curve* (AUC) was calculated to better evaluate the results. The larger AUC, the better classification ability of the system.

In both applications the system accuracy reached about 95% (human), 97% (canine), its sensitivity about 92% while specificity 99%. The detailed results achieved for different training and testing sets were averaged over the testing subsets and gathered in Table 1 and in Table 2.

Based on TPR and TNR measures, the classifier performance is also checked by the receiver operating characteristic. Fig. 7 presents the ROC curves of the classifier trained and tested on human blood cells (blue line) as well as the classifier trained and tested on canine blood cells

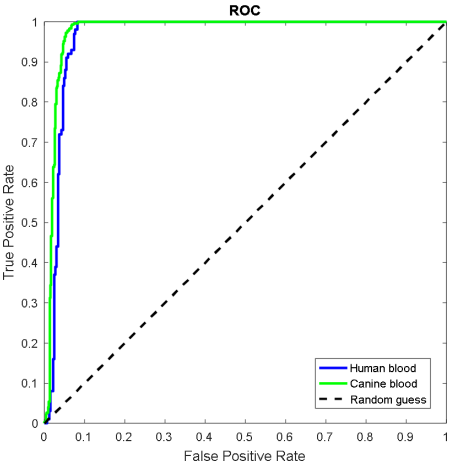

Fig. 7. Receiver operating characteristic curves of the classification system. Human blood test sets (blue), canine blood test sets (green), random guessing (dotted).

Table 1. The human red blood smear analysis results obtained with the decision-support system.

Evaluation criteria	Result	Number of analyzed red blood cells
Area under the curve (AUC)	94.79%	3200
Accuracy (ACC)	94.56%	3200
Specificity (TNR)	100.00%	1600
Sensitivity (TPR)	89.13%	1600

Table 2. The canine red blood smear analysis results obtained with the decision-support system.

Evaluation criteria	Result	Number of analyzed red blood cells
Area under the curve (AUC)	97.66%	2160
Accuracy (ACC)	96.34%	2160
Specificity (TNR)	97.70%	1080
Sensitivity (TPR)	93.98%	1080

(green line). The black dotted line represents random guessing. The ROC curves were created by taking the average of the charts of every k-fold test set. Notice that the classifier in both applications is very explicit.

4. Discussion and conclusion

The research has shown the influence of nanodiamond solutions on the red blood cell morphology leading to the cells' crenation – echinocytes. In order to automate the process of smear blood examination, the authors proposed a data-driven, intelligent decision-support system. The carried out studies showed benefits of using a computer-aided vision inspection of blood smears.

The applied optical measurement system coupled with advanced image processing techniques, multivariate statistical (eigenfaces) and intelligent algorithms (neural networks) produced good results of RBCs' separation, counting and finally classification. The advantages of such methods compared with a human operator are: short time of analysing large amounts of data, their repeatability and objectivity. On the other hand, these methods are data-driven, hence their effectiveness depends on the quality and the amount of the training data, therefore their design and validation should be supported and supervised by the medical specialists.

The system was examined in two case studies, the canine and human blood interacting with incubated nanodiamonds. Because of a specific nature of the considered problem, namely strong imbalance between erythrocytes and echinocytes in the databases, a number of blood cells were additionally created by skilful rotation of selected original cells, in order to increase and balance the databases.

The system estimated about 1.8% of echinocytes in the analysed human blood smears and about 1% in the canine blood ones, which is a negligible amount. In both applications the system accuracy reached 96%, with sensitivity of about 90% (human), 94% (canine) and specificity at the level of 99%, which are significantly better results comparing with those obtained in similar studies within this area. The results were afterwards consulted and accepted by the experienced medicine specialists.

The eigenfaces method used during the preprocessing stage as well as neural networks used in the classification stage, enable the system functionality to be easily extended onto other types of RBC abnormalities, *e.g.* spherocytes, stomatocytes, acanthocytes, what would not be possible with the use of simpler shape-feature analysers. However, the above mentioned applications require in-depth blood tests carried out on a much larger number of patients, which is actually the goal of the authors' work in the future.

Acknowledgements

Authors MF, MSW, and MJSZ acknowledge the DS funds of Department of Metrology and Optoelectronics, Faculty of Electronics, Telecommunications and Informatics, Gdańsk University of Technology. MSW acknowledges the support of National Science Centre under grant no. 2016/20/T/ST7/00380, and Foundation for Polish Science (FNP) START 95.2017. This study was partly supported by the Leading National Research Centre Scientific Consortium "Healthy Animal-Safe Food" Faculty of Veterinary Medicine, Warsaw University of Life Sciences, Poland. MG and AM acknowledge the DS funds of Department of Electrical Engineering, Control Systems and Informatics, Faculty of Electrical and Control Engineering, Gdańsk University of Technology. Furthermore, the authors would like to thank Mrs Magdalena Cymerman, Laboratory of Veterinary Analysis, ALAB Plus, for quality control of Good Laboratory Practices according to ISO17025 during the research work.

Authors' contributions: MG and MJSZ conceived the idea. MG and AM designed, implemented and tested the decision support system; MSW and MW performed the experiments; MW and MK analysed the data; MF prepared and provided the nanodiamonds. All authors wrote the paper.

References

[1] Provan, D. (2018). *ABC of Clinical Haematology 4ed*. Wiley Blackwell.

[2] Moritz, A., Fickenscher, Y., Meyer, K., Failing, K., Weiss, D.J. (2004). Canine and feline hematology reference values for the Advia 120 hematology system. *Vet Clin. Pathol.,* 33, 32–38.

[3] Walker, H.K., Hall, W.D., Hurst, J.W. (1990). *Peripheral blood smear, Clinical Methods: The History, Physical, and Laboratory Examinations.* Butterworths, Boston.

[4] Bhagavathi, S.L., Thomas Niba, S. (2016). An Automatic System for Detecting and Counting RBC and WBC using Fuzzy Logic. *ARPN Journal of Engineering and Applied Sciences*, 11(11), 6891–6894.

[5] Alomari, Y.M., Abdullah, S., Huda S.N., Zaharatul Azma, R., Omar, K. (2014). Automatic detection and quantification of WBCs and RBCs using iterative structured circle detection algorithm. *Computational and mathematical methods in medicine*, 1–17.

[6] Savkare, S.S., Narote S.P., (2015). Blood cell segmentation from microscopic blood images. *Information Processing (ICIP), International Conference on IEEE*, 502–505.

[7] Liu, Z., Liu, J., Xiao, X., Yuan, H., Li, X., Chang, J., Zheng, C., (2015). Segmentation of white blood cells through nucleus mark watershed operations and mean shift clustering. *Sensors*, 15(9), 22561–22586.

[8] Khajehpour, H., Dehnavi, A.M., Taghizad, H., Khajehpour, E., Naeemabadi, M. (2013). Detection and Segmentation of Erythrocytes in Blood Smear Images Using a Line Operator and Watershed Algorithm. *Journal of Medical Signals and Sensors*, 3(3), 164–171.

[9] Rawat, J., Singh, A., Bhadauria, H.S., Virmani, J. (2015). Computer aided diagnostic system for detection of leukemia using microscopic images. *Procedia Computer Science*, 70, 748–756.

[10] Zhang, C., Xiao, X., Li, X., Chen, Y.-J., Zhen, W., Chang, J., Zheng, C., Liu, Z. (2014). White Blood Cell Segmentation by Color-Space-Based K-Means Clustering. *Sensors*, 14, 16128–16147.

[11] Rosado, L., da Costa, J.M.C., Elias, D., Cardoso, J.S. (2017). Mobile-Based Analysis of Malaria-Infected Thin Blood Smears: Automated Species and Life Cycle Stage Determination. *Sensors*, 17, 2167.

[12] Spigulis, J. (2017). Multispectral, Fluorescent and Photoplethysmographic Imaging for Remote Skin Assessment. *Sensors*, 17, 1165.

[13] Kharbach, A., Bellach, B., Rahmoune, M., Rahmoun, M., Kacem, H.H. (2017). Towards a Novel Approach for Tumor Volume Quantification. *J. Imaging*, 3, 41.

[14] Hill, J. Matlock, K., Nutter, B., Mitra, S. (2015). Automated Segmentation of MS Lesions in MR Images Based on an Information Theoretic Clustering and Contrast Transformations. *Technologies*, 3, 142–161.

[15] Jędrzejewska-Szczerska, M. (2014). Response of a New Low-Coherence Fabry-Perot Sensor to Hematocrit Levels in Human Blood. *Sensors*, 14, 6965–6976.

[16] Jędrzejewska-Szczerska, M., Gnyba, M. (2011). Optical investigation of hematocrit level in human blood. *Acta Physica Polonica A*, 4, 642–646.

[17] Wierzba, P., Jędrzejewska-Szczerska, M. (2013). Optimization of a Fabry-Perot Sensing Interferometer Design for an Optical Fiber Sensor of Hematocrit Level. *Acta Physica Polonica, A*, 124(3), 586–588.

[18] Turk, M., Pentland, A. (1991) Eigenfaces for recognition. *Journal of Cognitive Neuroscience*, 3(1), 71–86.

[19] Kwasigroch, A., Mikołajczyk, A., Grochowski, M. (2017). Deep convolutional neural networks as a decision support tool in medical problems – malignant melanoma case study. *Advances in Intelligent Systems and Computing*, Springer International Publishing AG, Cham (ZG), 577, 848–856.

[20] Mikołajczyk, A., Kwasigroch, A., Grochowski, M. (2017). Intelligent system supporting diagnosis of malignant melanoma. *Advances in Intelligent Systems and Computing*, Springer International Publishing AG, Cham (ZG), 577, 828–837.

[21] Kwasigroch, A., Mikołajczyk, A., Grochowski, M. (2017). Deep neural networks approach to skin lesions classification – A comparative analysis. *22nd International Conference on Methods and Models in Automation and Robotics (MMAR)*, Międzyzdroje, Poland, 1069–1074.

[22] Swędrowski L., Duzinkiewicz, K., Grochowski, M., Rutkowski, T. (2014). Use of neural networks in diagnostics of rolling-element bearing of the induction motor. *Key Engineering Materials*, 588, 333–342.

[23] Wąsowicz, M., Ficek, M., Wróbel, M.S., Chakraborty, R., Fixler, D., Wierzba, P., Jędrzejewska-Szczerska, M. (2017). Haemocompatibility of Modified Nanodiamonds. *Materials*, 10(4), 352.

[24] Bain, B.J., Lewis, S.M., (2012) Preparation and staining methods for blood and bone marrow films. *Dacie and Lewis, Practical Hematology*, Elsevier: Edinburgh, UK, 57–68.

[25] Hübl, W., Andert, S., Erath, A., Lapin, A., Bayer, P.M. (1995). Peripheral blood monocyte counting: towards a new reference method. *Eur. J. Clin. Chem. Clin. Biochem.*, 33(11), 839–845.

[26] Walker, H.K., Hall, W.D., Hurst, J.W. (1990). Peripheral blood smear, Clinical Methods: The History, Physical, and Laboratory Examinations. Butterworths, Boston, 155.

[27] Jackson, J.E. (1991). *A User's Guide to Principal Components*. Wiley.

[28] Nowicki A., Grochowski, M. (2011). *Kernel PCA in Application to Leakage Detection in Drinking Water Distribution System, Computational Collective Intelligence*. Technologies and Applications, Springer Berlin Heidelberg, 497–506.